

# The Role of Spin – Orbit Coupling in the Spin Transport FM-(G/C)N-FM

Mohannad M. Merzoq\*<sup>1</sup>, Jenan M. Al-Mukh<sup>2</sup>

<sup>1&2</sup>Department of Physics, College of Education for Pure Sciences, University of Basrah, Basrah, Iraq.

**Abstract** The spin transport through DNA system formed by a guanine-cytosine is studied extendedly in our work. Hence, theoretical treatment is accomplished for one magnetized active region (includes base pairs and backbone) coupled to ferromagnetic leads in parallel configuration case, throughout magnetic quantum contacts (FM-(G/C)N-FM). Our treatment is based on the tight binding model to derive obvious formula for the spin dependent transmission spectrum which is employed to investigate the spin transport through DNA junction. Our calculations are accomplished in the presence of spin-orbit coupling for strong, weak and "without backbone" regimes. The role the system spin dependent factors of the transport of (G/C)N molecule are investigated in our study. These factors include the molecular length, as well as externally applied bias voltage. Variation of these factors can enhance or suppress spin transport through (G/C)N molecule (with N=10,15,20,25). The transmission spectrum results confirm that the spin transport throughout (G/C)N is originated by a coherent tunneling process between neighboring bases through the overlapping of the LUMO orbitals of the bases. The physical mechanism is raised from quantum interference combination with molecular length and the presence of spin-orbit coupling. The best functional feature for environmental effect, which may induce dephasing such as leads temperature, is investigated. The results showed that the spin-polarized transport can be effectively regulated by the molecular length of (G/C) which can exhibit efficient spin filtering and spin switching



 Crossref  [10.36371/port.2024.special.3](https://doi.org/10.36371/port.2024.special.3)

**Keywords:** Spin transport, DNA junction, Spin-polarized.

## 1. INTRODUCTION

Microscopic and macroscopic models have been established to quantitatively calculate the charge transport in DNA[2]. The use of single molecules as functional devices is the ultimate end of the ongoing trend toward the miniaturization of electronic circuits[3]. Three types of electron transfer mechanisms typically have been explored, incoherent hopping, coherent super exchange and partially coherent hopping transport.

Since spin is not a conserved quantity in solids due to spin-orbit and hyperfine coupling spin decoherence mechanisms in metals and semiconductors, spin transport is different from charge transport. The spin-orbit interaction (SOI) had been extensively studied in order to build microstructures and crystals with the spin polarization needed in nonmagnetic environments. Modest SOI is one of the difficulties that organic spintronics must overcome. Light-element atoms, like carbon and oxygen, which make up organic molecules, have modest SOI. Therefore, it was traditionally believed that organic compounds had a low efficiency for producing spin polarization. Contrary to such a preconception, a high efficiency of spin filtering, comparable to the highest efficiency in other systems, has been discovered in helical organic molecules such as double-stranded DNA. Spintronics in DNA may lead to nanoscale quantum computation. The spin transport properties of the DNA (as an organic molecule) make it

applicable as a spintronics device. Rich physics behind the organic materials and specific functions (such as switch ability with light and electrical or magnetic fields) are two important motivations for using the organic materials in spintronics applications [4].

Experimental advances include the demonstration of conductance, switching, rectification, negative differential conductance and other promising phenomena beyond simple electron transport, such as quantum interference, thermoelectricity and optoelectronics spintronics. Detailed measurements had been reached that a short DNA molecule is a one-dimensional conductor and can be used as molecular wires [5-9].

By using a tight-binding model, it was predicted that spin transport could be observed in short DNA molecules sandwiched between ferromagnetic contacts[10]. It was shown that a DNA spin valve can be realized with magnetoresistance values of 26% for Ni and 16% for Fe contacts. By merging density-functional theory based calculations and model Hamiltonian approaches, DNA quantum transport (during the stretching-twisting process of poly(GC) DNA) had been studied [11]. The conflict between stretching and twisting during the stretching process results in local maxima in the charge transfer integral between two nearest-neighbor GC pairs. Most of the development in

spintronics is currently based on inorganic materials. The spin selectivity of organic based spintronics devices originated from an inorganic ferromagnetic electrode and was not determined by the organic molecules themselves. It showed that conduction through double-stranded DNA is spin selective, demonstrating a true organic spin filter[12]. A Hall device was used to monitor the spin polarization of electrons that are either reorganized inside the molecules or transferred across the self-assembled monolayers of DNA adsorbed on the device surface. [5]. It was able to see charge transport and spin-dependent charge polarization across double-stranded DNA with oxidative damage and at different lengths. The spin-dependent transport across oxidatively damaged DNA was seen to be enhanced.

In this paper, an apparent physical model for spin-dependent phenomena is described providing a physical model to analyze spin transport across DNA system. Tight binding model is used to achieve our model calculations. The system under consideration consists of two ferromagnetic leads connected to the DNA bases guanine and cytosine (FM-(G/C)N-FM). The main purpose in our study is to investigate the electronic and

the spin transport properties of (FM-(G/C)N-FM) taken into account the DNA molecular structure, the quantum connection of molecule with lead and the spin-orbit coupling interaction.

## 2. THEORETICAL MODEL

In our treatment, the tight binding model is used for the DNA stack which can be constructed as a one dimensional model. There is a single central conduction channel in which individual sites represent the base-pair and backbone. Every link between sites implies the presence of a coupling interaction. The description of DNA base pair as a single site represents a simplification of the wire model. We describe the system under consideration by spin-dependent Hamiltonian (using Dirac's notations). This electronic Hamiltonian takes into account all the spin dependent sub-systems interactions. The different indexes D, A, a, L and R denote the donor, acceptor, the bridge (the active region DNA molecules bases with total number N) and the left and right leads. By using the tight binding model the spin dependent Hamiltonian model for certain spin is written as follows:

$$\begin{aligned} \hat{H} = & \sum_{k_L} E_{k_L}^\sigma |k_L\sigma\rangle\langle k_L\sigma| + E_D^\sigma |D\sigma\rangle\langle D\sigma| + \sum_{k_a} E_{k_a}^\sigma |k_a\sigma\rangle\langle k_a\sigma| + E_A^\sigma |A\sigma\rangle\langle A\sigma| + \sum_{k_R} E_{k_R}^\sigma |k_R\sigma\rangle\langle k_R\sigma| \\ & + \sum_{k_L} [V_{Dk_L}^\sigma |D\sigma\rangle\langle k_L\sigma| + V_{k_L D}^\sigma |k_L\sigma\rangle\langle D\sigma|] + \sum_{k_a} [V_{Dk_a}^\sigma |D\sigma\rangle\langle k_a\sigma| + V_{k_a D}^\sigma |k_a\sigma\rangle\langle D\sigma|] \\ & + \sum_{k_a} [V_{Ak_a}^\sigma |A\sigma\rangle\langle k_a\sigma| + V_{k_a A}^\sigma |k_a\sigma\rangle\langle A\sigma|] + \sum_{k_R} [V_{Ak_R}^\sigma |A\sigma\rangle\langle k_R\sigma| + V_{k_R A}^\sigma |k_R\sigma\rangle\langle A\sigma|] \end{aligned} \quad (1)$$

The index  $k_i$  is the energy wave vector, with  $i$  represents the indexes D, A, a, L and R.  $E_i^\sigma$  represents the  $i$ th energy level position and spin.  $|i\sigma\rangle$  and  $\langle j\sigma|$  represent the ket and bra states, respectively.  $V_{ij}$  represents the coupling interaction between the subsystems  $i$  and  $j$  with  $V_{ij} = V_{ji}$ . The system time dependent and spin dependent wave function can be written as,

$$\Psi^\sigma(t) = C_D^\sigma(t)|D\sigma\rangle + C_A^\sigma(t)|A\sigma\rangle + \sum_{k_a} C_{k_a}^\sigma(t)|k_a\sigma\rangle + \sum_{k_L} C_{k_L}^\sigma(t)|k_L\sigma\rangle + \sum_{k_R} C_{k_R}^\sigma(t)|k_R\sigma\rangle \quad (2)$$

Where  $C_j^\sigma(t)$  represents the linear expansion coefficients, with  $j=D,A,a,L$  and  $R$ . The equations of motion for  $C_j^\sigma(t)$  can be obtained by using time dependent Schrodinger equation [13] (in atomic units):  $\frac{d\Psi^\sigma(t)}{dt} = -i\hat{H}\Psi^\sigma(t)$ . Accordingly, we get set of time dependent and spin dependent related equations. For steady state case  $C_j^\sigma(t)$  is defined as  $C_j^\sigma(t) = \bar{C}_j^\sigma(E^\sigma) e^{-iE^\sigma t}$  with  $E^\sigma$  represents the spin dependent system energy values. For steady state, we have  $\frac{dC_j^\sigma}{dt} = 0$  and by using the following separation procedure:  $V_{k_j\alpha}^\sigma = v_{k_j}^\sigma V_{\alpha}^\sigma$  and  $\bar{C}_{k_i}^\sigma = v_{k_i}^\sigma \bar{C}_i^\sigma$  Then, by using the following definition of the self-energy [14]

$$\sum_{ij}^\sigma(E^\sigma) = |V_{ij}^\sigma|^2 \Gamma_j^\sigma(E^\sigma) \quad (3)$$

where,

$$\Gamma_j^\sigma(E^\sigma) = -i\pi\rho_j^\sigma(E^\sigma) + P \int \frac{\rho_j^\sigma(E^\sigma) dE^\sigma}{E^\sigma - E^\sigma} \quad (4)$$

and the spin dependent density of states:

$$\rho_j^\sigma(E^\sigma) = \sum_{k_j} |v_{k_j}^\sigma|^2 \delta(E_{k_j}^\sigma - E^\sigma) \quad (5)$$

The, the energy dependent relations are treated to get : and,

$$\therefore \frac{\bar{C}_A^\sigma(E^\sigma)}{\bar{C}_D^\sigma(E^\sigma)} = \frac{\sum_{AaD}^\sigma(E^\sigma)}{E^\sigma - E_A^\sigma - \sum_{AR}^\sigma(E^\sigma) - \sum_{Aa}^\sigma(E^\sigma)} \quad (6)$$

Now, the spin dependent transmission amplitude and transmission probability can be, respectively, defined by:  

$$t^\sigma(E^\sigma) = \frac{C_A^\sigma(E^\sigma)}{C_B^\sigma(E^\sigma)} \quad (8); \text{ and } \tau^\sigma(E^\sigma) = |t^\sigma(E^\sigma)|^2.$$

$$E_j^\sigma = E_{\text{basis}} - 2t_{\text{bp}}^\sigma \cos\left(\frac{\pi j}{N+1}\right) \pm \sqrt{\left[t_{\text{bp}}^\sigma \cos\left(\frac{\pi j}{N+1}\right)\right]^2 + 2t_{\text{bb}}^2} + \sigma\Delta_s \quad (7)$$

Where  $j$  refers to a single base pair.  $E_{\text{basis}}$  is the energy of the basis (i.e the energy of one base pair).  $N$  represents the number of the base pairs. ( $t_{\text{bp}}$ ) is the coupling interaction between nearest-neighbor base pairs. (the coupling interaction between base pairs and backbone).  $\sigma (= \pm 1)$  refers to for spin up and spin down, respectively. ( $\Delta_s = 0.4\text{eV}$ ) represents the energy splitting due to magnetic field effect.

The enhancement of spin-orbit coupling due to chirality of DNA and Zeeman splitting of energy level spectrum in magnetic field parallel to the DNA axis are the main observations about the spin transport through DNA. In this work, the chiral feature will be considered taking into consideration small angle of chirality. In our calculation, the chirality will be considered by taken the spin-orbit coupling according to the following:  $E_j^\sigma \rightarrow E_j^\sigma + \lambda\Delta_{\text{so}}$ . Where,  $E_j^\sigma$  is given by eq.(7) and  $\Delta_{\text{so}}$  is the spin-orbit coupling with  $\lambda = \pm 1$ . In all our calculations, we demand the regime  $\Delta_s > \Delta_{\text{so}}$ .

### 3. CALCULATIONS AND RESULTS

Our calculations are accomplished for two regimes, the strong regime where  $t_{\text{bb}}^\sigma > t_{\text{bp}}^\sigma$  and the weak regime where  $t_{\text{bb}}^\sigma < t_{\text{bp}}^\sigma$ . The basepair-backbone coupling interactions for the upper and lower backbone sites (for certain spin) are considered in all our treatment to be equal.

The parameters used in our calculations for the case of strong regime are:  $t_{\text{bp}}^\sigma = 0.5\text{eV}$ ,  $t_{\text{bp}}^{-\sigma} = 0.25\text{eV}$ ,  $t_{\text{bb}}^\sigma = 0.7\text{eV}$  and  $t_{\text{bb}}^{-\sigma} = 0.35\text{eV}$ , while for the case of weak regime  $t_{\text{bp}}^\sigma = 0.7\text{eV}$ ,  $t_{\text{bp}}^{-\sigma} = 0.35\text{eV}$ ,  $t_{\text{bb}}^\sigma = 0.5\text{eV}$  and  $t_{\text{bb}}^{-\sigma} = 0.25\text{eV}$ . The coupling interactions between subsystems are  $V_{\text{AR}}^\sigma = 1.5\text{eV}$ ,  $V_{\text{AR}}^{-\sigma} = 0.75\text{eV}$ ,  $V_{\text{Aa}}^\sigma = 1.2\text{eV}$ ,  $V_{\text{Aa}}^{-\sigma} = 0.6\text{eV}$ ,  $V_{\text{Ad}}^\sigma = 0.5\text{eV}$  and  $V_{\text{Ad}}^{-\sigma} = 0.25\text{eV}$ . The energy levels of the acceptor quantum contact are  $E_A^\sigma = -0.2\text{eV}$  and  $E_A^{-\sigma} = 0.2\text{eV}$ . Zeeman energy  $\Delta_s$  equals to  $0.4\text{eV}$ . To accomplish our calculations the eigen values of the active region are calculated for the sequence (G/C)N for both regimes by using Eq.(7)  $E_{\text{basis}}$  is the energy of the basis i.e. the energy of one base pair  $E_{\text{basis}}$  equals to  $\left(\frac{E_G + E_C}{2}\right)$ .  $E_G (= -0.63\text{eV})$  and  $E_C (= -3.75\text{eV})$  are the onsite energies of Guanine and Cytosine, which are calculated with respect to  $E_F = -5.5\text{eV}$ .

The eigen values of the active region, that contains base pairs with backbone (when the base pairs arranged in homogenous sequence) will be calculated by using tight binding model [13]. in the presence of magnetic field and spin dependent coupling interaction between subsystem

All the electronic and transport properties will be calculated and studied for the case of leads in the parallel configuration.  $\mu_\alpha^\sigma$  represents the chemical potential of the lead  $\alpha (= L, R)$  for certain spin  $\sigma$  with  $\mu_L^\sigma = \mu_R^\sigma = 0.1\text{eV}$  and  $\mu_L^{-\sigma} = \mu_R^{-\sigma} = -0.1\text{eV}$ .  $E_A^\sigma(E_D^\sigma)$  represents the spin dependent energy levels of the acceptor (donor). For the strong, weak and without backbone regimes, the eigen values energies are calculated in the presence of spin-orbit coupling with  $\Delta_{\text{so}} = 0.2\text{eV}$ . These results are considered as the access to calculate the electronic and transport properties. According to these results, many features can be reported;

- 1- In the presence of spin-orbit coupling, the number of energy levels of the (G/C)N active region will increase with  $N$  to be  $4N$ .
- 2- Our results show that the eigen values are shifted to higher positive values of energy in the strong coupling regime for each  $N$  and for both spin. This shift in energy increases with the number of base pairs. For the without backbone regime, the eigen values are shifted to the positive higher energies and to the lower negative energies for both spin and each  $N$ . It is obvious that the eigenvalues concerned to the case of weak regimes are lying in energy range of the other regimes. These results are physically correct.

The eigen energy values are employed to calculate the spin dependent transmission spectrum in the strong coupling regime, where the coupling interaction between base pairs and backbone is greater than the coupling interaction between base pairs. Figs. (1) exhibit the transmission spectrum in the presence of spin-orbit coupling for different values of base pairs number,  $N = 10, 15, 20$  and  $25$ . For  $N = 10$ , the higher values of transmission coefficient are lying in the range  $0.6\text{eV} \leq eV_b \leq 2.1\text{eV}$  ( $0.935\text{eV} \leq eV_b \leq 1.40\text{eV}$ ) for spin up (spin down) channel.

For  $N = 15$ , the higher values of transmission coefficients lying in the bias voltage range at  $0.7\text{eV} \leq eV_b \leq 2.1\text{eV}$  for spin up channel. For spin down channel, there is clear reduction in the values of transmission coefficient, except two obvious Fano resonances. With increasing the number of base pairs, the number of resonances with high coefficient decreases remarkably for spin up channel. The same above mentioned

feature can be reported when  $N=20$  and  $25$  for spin down channel.

The spin dependent currents are also calculated and presented in fig. (2) for different values of  $N$ . These figures emphasizes that there is no certain role for the number of base pairs. The current shows three ranges of linear relationship in the spin up channel. While, wide spin blockade energy is shown in the spin down channel. This width is equal to  $0.8\text{eV}$ . In general  $I^\sigma \gg I^{-\sigma}$ , since  $I^{-\sigma}$  is nearly vanished  $-0.43\text{eV} \leq eV_b \leq 0.43\text{eV}$ . The temperature conductance dependence, for different values of  $N$  is shown in Fig. (3). This Figures shows that  $G^\sigma \gg G^{-\sigma}$ , where  $G^\sigma(G^{-\sigma})$  decreases (increases) with  $T$ . These results show that there is no role for the spin down channel.

The transmission spectrum, in the weak regime for different values of  $N$ , is calculated and presented in fig. (4) In the presence of spin-orbit coupling, the number of resonances are nearly  $2N$  for each spin. Most of them are, Fano resonances, shifted towards higher energies especially for spin up channel. The values of spin up transmission resonances are higher than the spin down resonances But when the number of base pairs increases, the transmission values become obviously lower especially for spin down channel. These features will certainly determine the transport properties of the DNA active region. The spin currents dependence are presented in Figs. ((5)). For  $N \geq 10$ , we notice the same physical features, where  $I^\sigma_{eV_b}$  show asymmetric feature with bias voltage polarity in the spin up channel. For the spin down channel, it is noticed that the width of spin down blockade voltage is shifted to the positive values of bias voltage with width equals to  $0.6\text{eV}$ . In this regime, no role for the number of base pairs is exhibited. According to our electronic properties calculations, the temperature-conductance dependence shows different spin dependent features. see Fig (6), where  $G^\sigma > G^{-\sigma}$ . In the spin up channel, no role for the number of base pairs, is found in the conductance, for  $T > 240\text{K}$ . While, in the spin down channel,  $G^{-\sigma}$  is vanished for  $T < 240\text{K}$  and For  $T > 240\text{K}$ , the conductance increases tardily with temperature.

For case of without backbone regime, our results can be summarized by the following:

1. Almost the higher transmission coefficient are Fano resonances for all  $N$  and both spin (see Figs (13-16). Nearly, These resonances are lying in system energy higher than  $0.7\text{eV}$ . The lower values of transmission coefficients are noticed when  $N=25$  in the spin down channel.

2. Figs (17) show the current-bias voltage linear relation of the spin up channel for different base pairs number. Notably, the current. equals zero at  $eV_b = -0.1\text{eV}$ . While, for spin down channel, the lower values of current are lying in the range  $0 < eV_b < 0.2\text{eV}$ . The spin down current shows very narrow spin blockade width equals to  $0.076\text{eV}$  for all  $N$ .
3. The calculation of conductance-temperature dependence is shown in Fig.(18), where  $G^\sigma > G^{-\sigma}$ . For  $N \geq 20$ ,  $G^\sigma$  is constant with temperature variation. For  $N < 20$ ,  $G^\sigma$  decreases with temperature. In the spin down channel,  $G^{-\sigma} = 0$  for all  $N$  and  $T \leq 160\text{K}$ , while for  $T > 160\text{K}$ ,  $G^{-\sigma}$  increases with  $T$ .

#### 4. CONCLUSIONS

In our study, we investigate the effect of electron spin on the electron transport through a certain number of base pairs when exposed to the variations of the coupling between (FM-(G/C)N-FM) subsystems, ie the spin dependent quantum contacts and leads and the effect of backbone. The spin transport properties through (G/C)N are evaluating numerically. The on-site energy in our study are fixed for all subsystems. In relation to the spin dependent feature applications, we dealt with several parameters associated with the experimental works. (G/C)N sequences have been employed to determine the spin transmission and  $I^\sigma_{eV_b}$  characteristic in the absence and presence of spin-orbit coupling.

Our results that summarized by the following have described various features of the (G/C)N molecules; Strong regime:  $I^\sigma$  has linear relation with  $eV_b$ ,  $I^{-\sigma}$  has not narrow spin blockade width both are symmetric about  $eV=0$ ;  $I^\sigma > I^{-\sigma}$ . Weak regime:  $I^\sigma$  is linear with  $eV_b$ , shifted to the negative  $eV_b$  bias voltage.  $I^{-\sigma}$  shows spin blockade, shifted to the positive  $eV_b$ ;  $I^\sigma > I^{-\sigma}$ . Without backbone: is linear with  $eV_b$ , shifted to the negative  $eV_b$  bias voltage.  $I^{-\sigma}$  shows spin blockade, shifted to the positive  $eV_b$ ;  $I^\sigma > I^{-\sigma}$ .

Our calculations include the characteristics of the structures and their relevance to the spin transport properties. We found that the spin-polarized current could rapidly increase under it a small bias voltage by tuning the coupling interactions between the subsystems well as the (G/C)N molecule can be tuned to act as a semiconductor. Our results show that increasing the molecular length may enhance noticeably same of electric and transport properties.

We also focused our attention to the impact of temperature on the spin transport properties. Increasing temperature may cause the destruction of the phase coherence and may lead to the reduction of conductance.

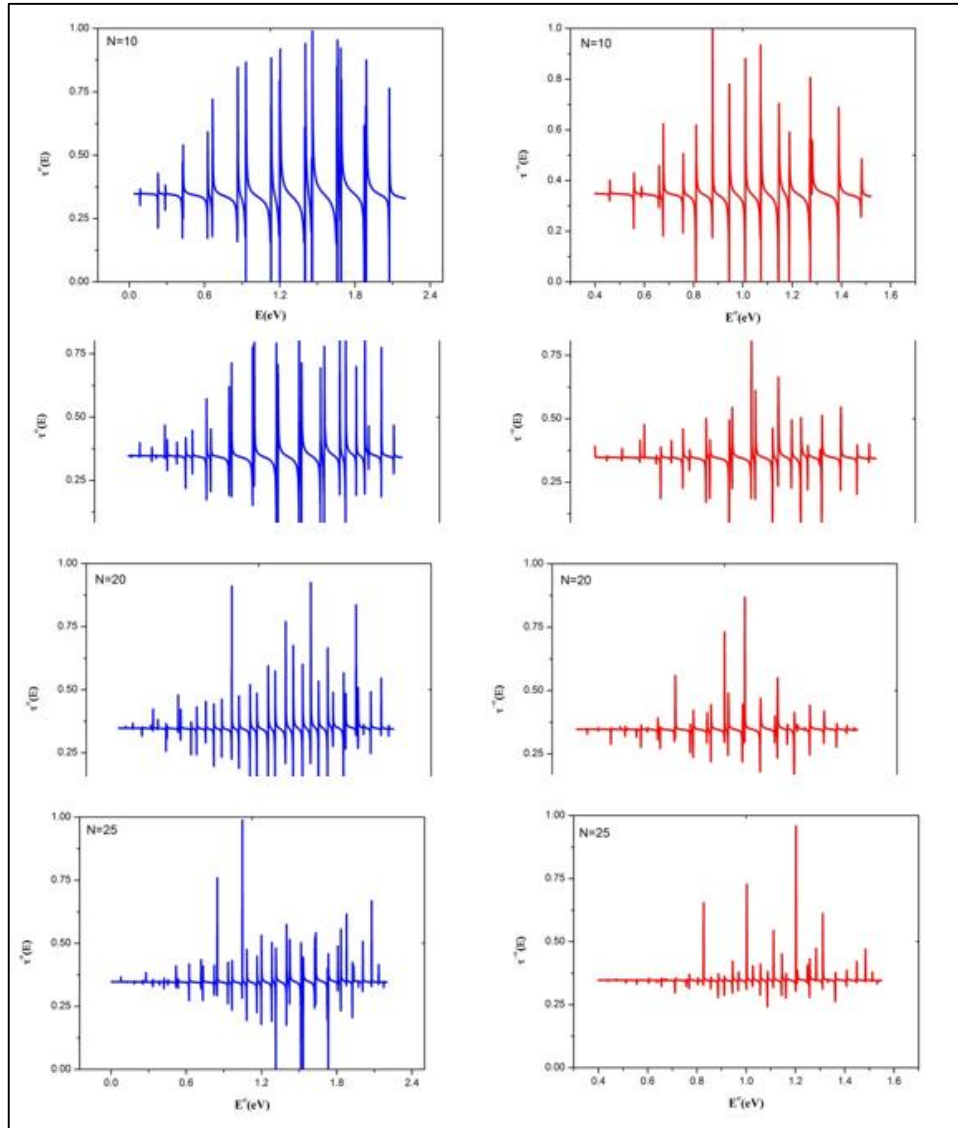


Fig (1):  $\tau^\sigma$  and  $\tau^{-\sigma}$  spectrum for the strong regime in the presence of spin – orbit coupling for different of  $N$ .

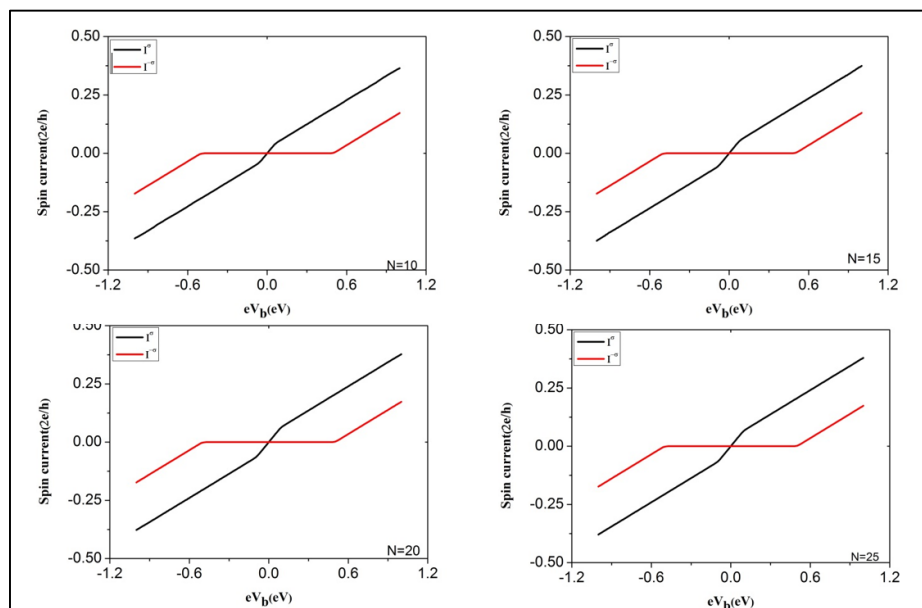


Fig.(2):  $I^\sigma$  and  $I^{-\sigma}$  as a function of bias voltage for the strong regime in the presence of spin – orbit coupling for different values of  $N$ .

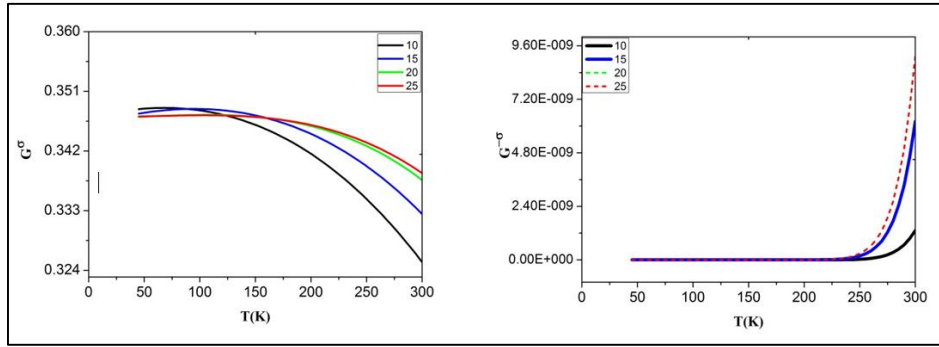


Fig.(3):  $G^\sigma$  and  $G^{-\sigma}$  as a function of temperature for the strong regime in the presence of spin – orbit coupling for different of  $N$ .

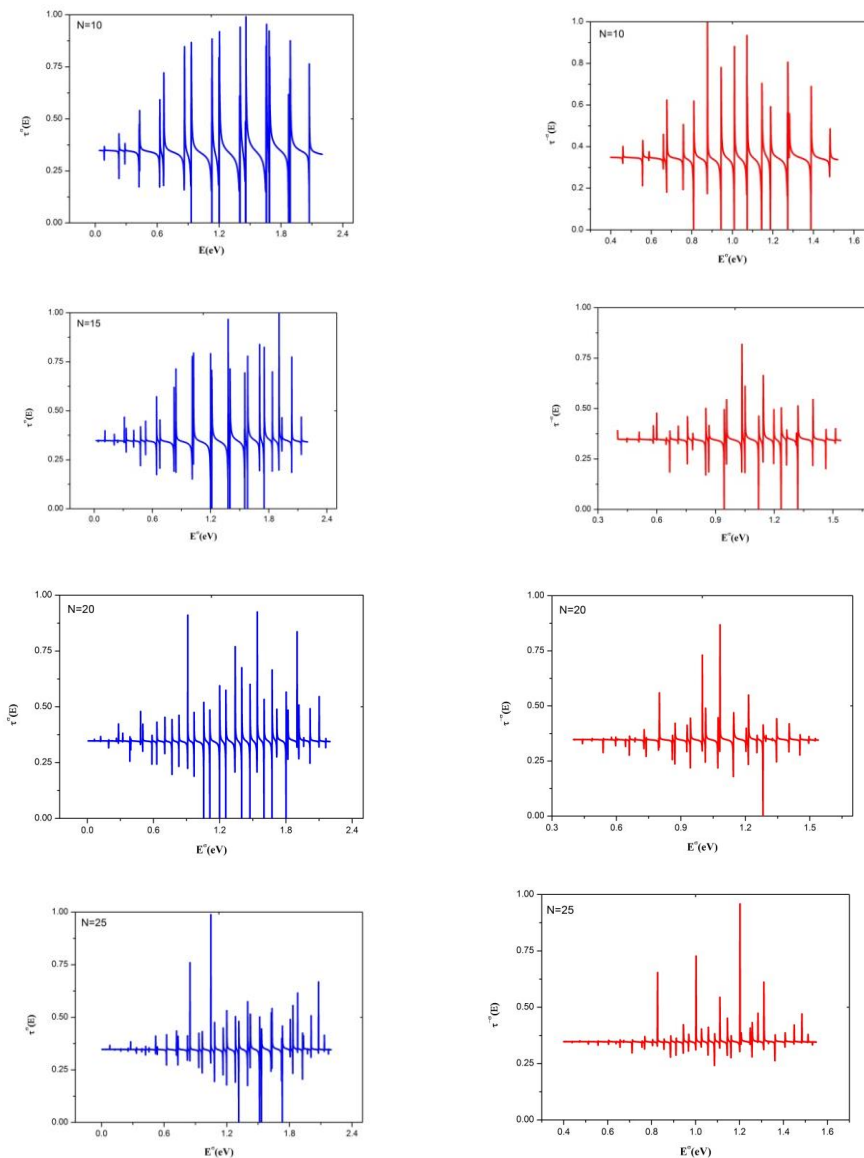


Fig (1):  $\tau^\sigma$  and  $\tau^{-\sigma}$  spectrum for the strong regime in the presence of spin – orbit coupling for different of  $N$ .

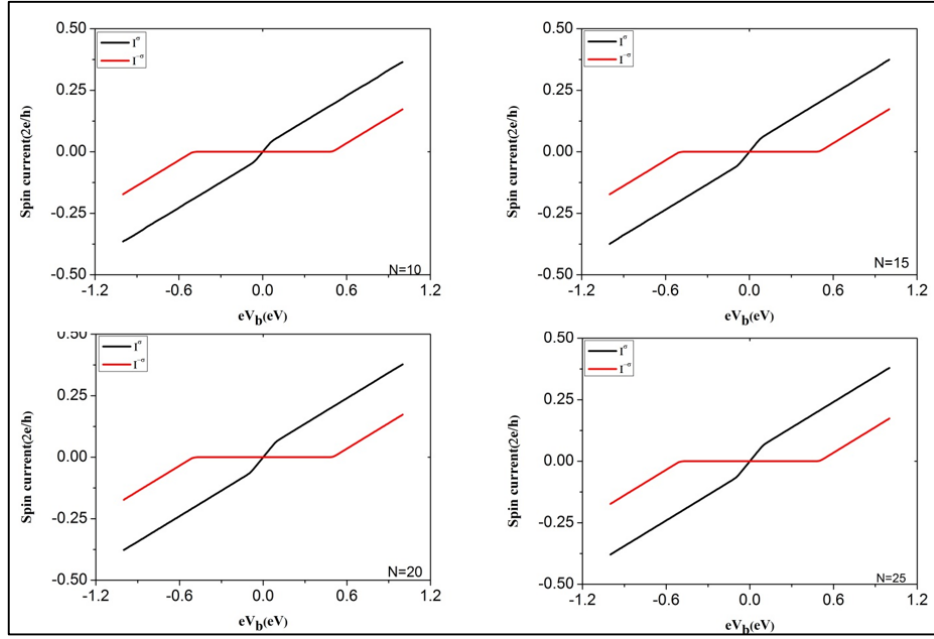


Fig.(2):  $I^\sigma$  and  $I^{-\sigma}$  as a function of bias voltage for the strong regime in the presence of spin – orbit coupling for different values of  $N$ .

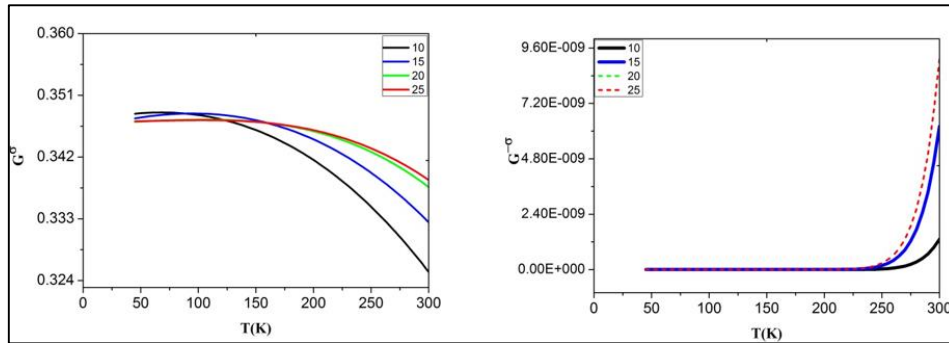
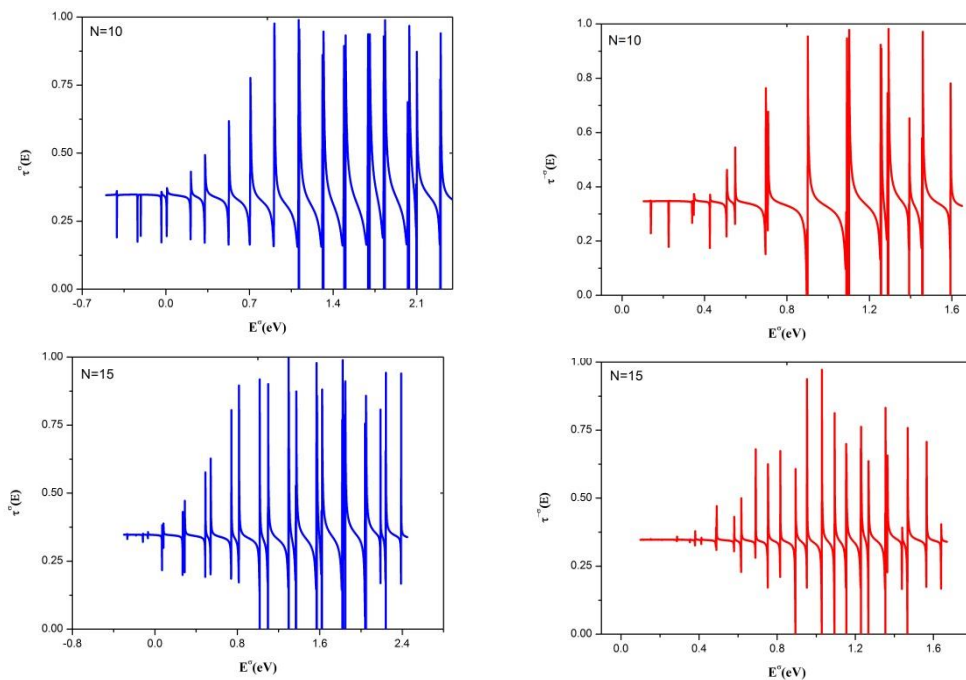


Fig.(3):  $G^\sigma$  and  $G^{-\sigma}$  as a function of temperature for the strong regime in the presence of spin – orbit coupling for different of  $N$ .



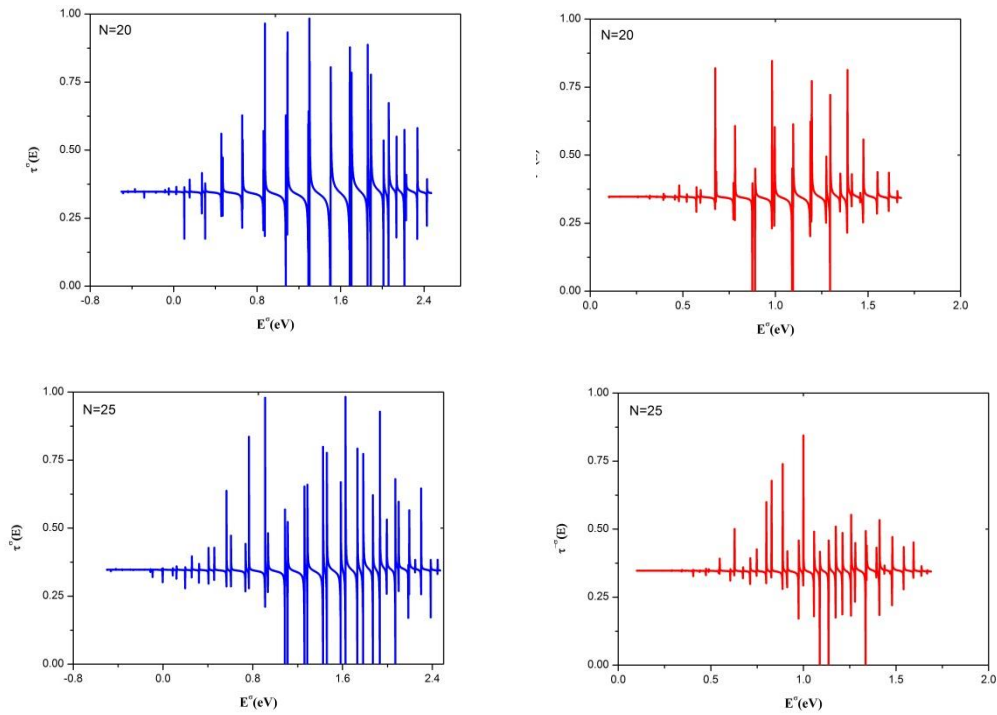


Fig (4):  $\tau^\sigma$  and  $\tau^{-\sigma}$  spectrum for the weak regime in the presence of spin – orbit coupling for different values of  $N$ .

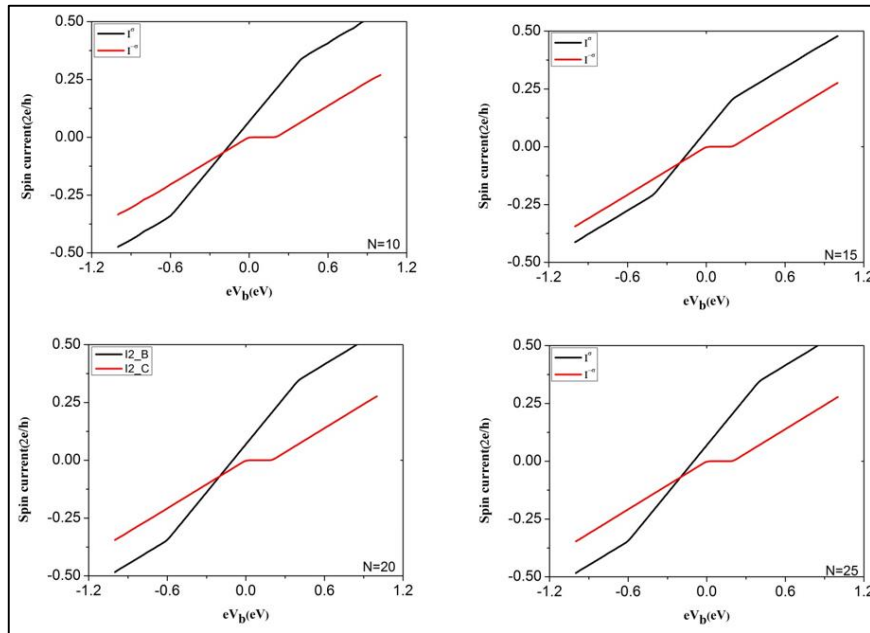


Fig.(5):  $I^\sigma$  and  $I^{-\sigma}$  as a function of bias voltage for the weak regime in the presence of spin – orbit coupling for different values of  $N$ .

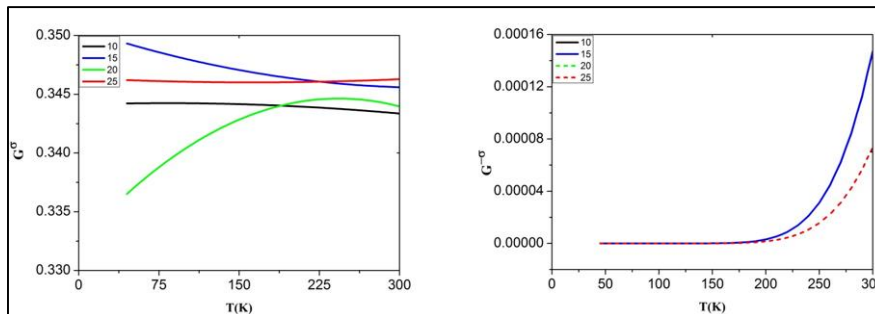


Fig.(6):  $G^\sigma$  and  $G^{-\sigma}$  as a function of temperature for the weak regime in the presence of spin – orbit coupling for different values of  $N$ .

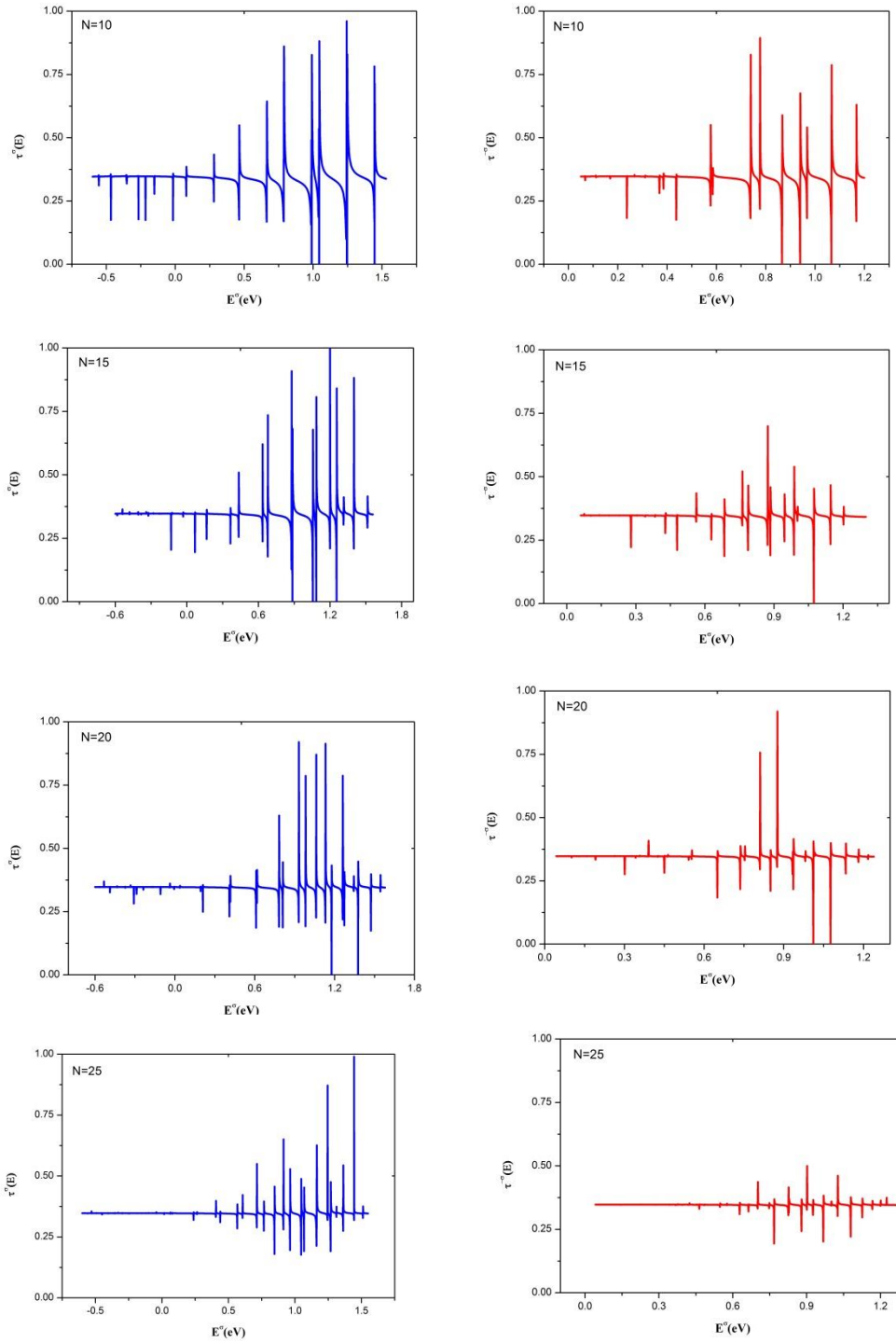


Fig (7) :  $\tau^\sigma$  and  $\tau^{-\sigma}$  spectrum for the without backbone regime in the presence of spin – orbit coupling for different values of  $N$ .

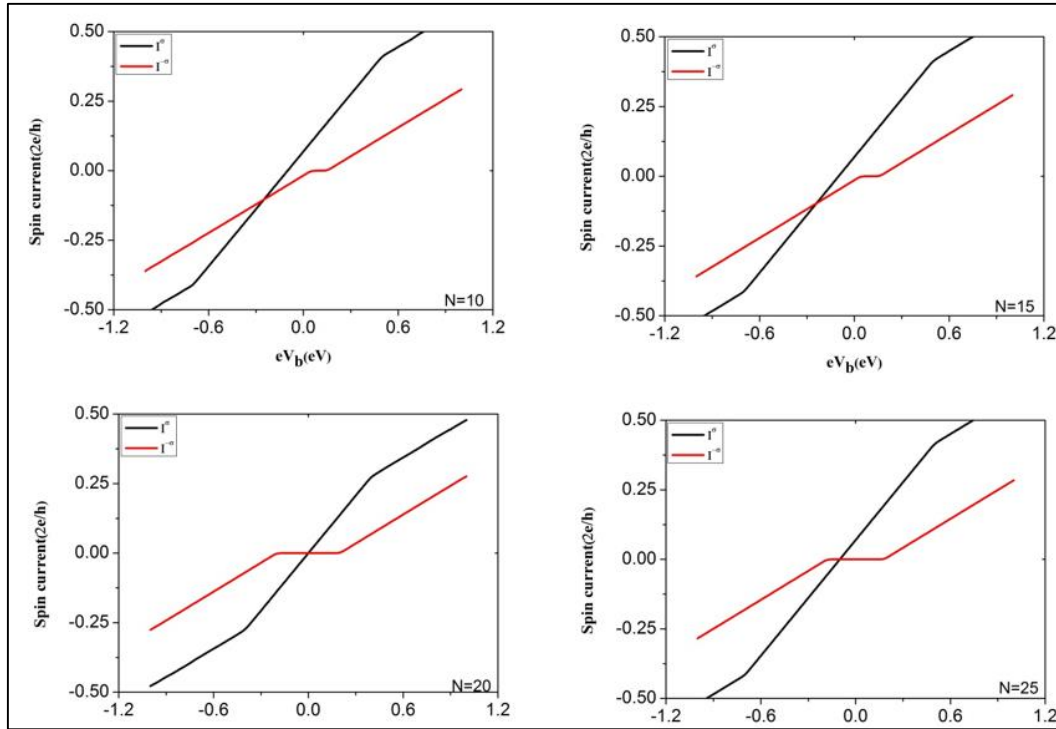


Fig.(8):  $I^\sigma$  and  $I^{-\sigma}$  as a function of bias voltage for the without backbone regime in the presence of spin – orbit coupling for different values of  $N$ .

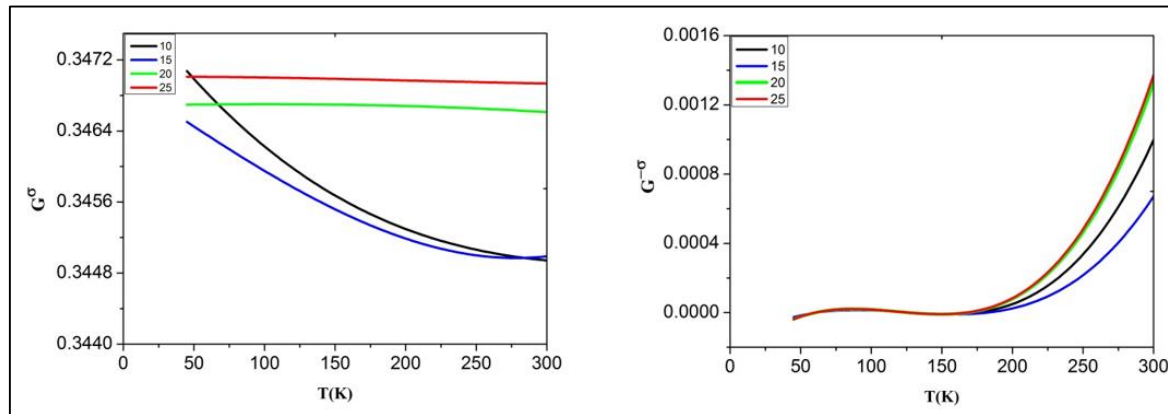


Fig.(9):  $G^\sigma$  and  $G^{-\sigma}$  as a function of temperature for without backbone in the presence of spin – orbit coupling ( $G/C$ ) $N=10,15,20,25$ .

## REFERENCES

- [1] K. Wang, E. Meyhofer,\* and P. Reddy “Thermal and Thermoelectric Properties of Molecular Junctions,” Adv. Funct. Mater, vol. 30, no. 8, (2020).
- [2] S. Al-Saidi, J. Al-Mukh, S. I. Easa , “Steady State Formalism for Electron Transfer through DNA System: Fishbone Model,” IJSR, vol. 3, no. 10, (2014).
- [3] S. H. Ke, Y. Weitao, and H. U. Baranger, “Quantum-interference-controlled molecular electronics,” Nano Lett, vol. 8. (2008).
- [4] S. Al-Saidi, J. Al-Mukh, and S. I. Easa. “Investagations in the Physical Features of Electron Transfer Process through DNA System,” Ph. D. dissertation, University of Basrah, Iraq, (2015).
- [5] J. Artés, Y. Li, J. Qi, and M. Anantram, “Conformational gating of DNA conductance,” Nat comm, vol. 9, (2015).

- [6] C. Zhang, H. Yao, and Y. Nie, “Non-equilibrium quantum transport of spin-polarized electrons and back action on molecular magnet tunnel-junction,” *AIP Advance*, vol. 9, (2016).
- [7] S. Abdalla, A. Obaid, and F. M. Al-Marzouki, “Effects of Environmental Factors and Metallic Electrodes on AC Electrical Conduction Through DNA Molecule,” *Nanoscale Res Lett*, vol. 12, (2017).
- [8] S. K. Jr, and L. K.-E. “Electron transfer in superlattice films based on self-assembled DNA-Gold nanoparticle,” *ACS Nano*, vol.31, (2019).
- [9] M. Sierra, D. Sánchez, and R. Gutierrez, “Spin-polarized electron transmission in DNA-like systems,” *Biomolecules*, vol.10, (2019).
- [10] M. Zwolak, and M. D. “DNA spintronics,” *Applied Phys Lett*. Vol. 81, (2002).
- [11] A. Storm, J. van Noort, and S. de Vries, “Insulating behavior for DNA molecules between nanoelectrodes at the 100 nm length scale,” *Nanoscale Res Lett*, vol. 79, (2001).
- [12] N. Bangruwa, M. Srivastava, D. M.- Magnetochemistry, “Radiation-Induced Effect on Spin-Selective Electron Transfer through Self-Assembled Monolayers of ds-DNA,” *Magneto chem*, vol, 7,no. 98, (2021).
- [13] D. Klotsa, R. A. Ro`mer, and M. S. Turner, "Electronic Transport in DNA" *Biophysical Journal*, Vol. 89, (2005).
- [14] M. A. Najdi, J. M. AL-Mukh, and H. A. Jassem, “Heat current across double quantum dots in series coupled to ferromagnetic leads in antiparallel configuration within weak interdot coupling regime,” *J Comput Electron*, Vol. 20, (2021).